

CAVITATION CHARACTERISTICS OF RESTRICTION ORIFICES (Experiment for Shock Pressure Distribution by Cavitation on Restriction Orifices and Occurrence of Cavitation at Multiperforated Orifices due to Interference of Butterfly Valve)

Kei Takahashi and Hiroyuki Matsuda
Chiyoda Corporation, Yokohama, JAPAN

Hirofumi Miyamoto
Chitose Institute of Science and Technology, Hokkaido, JAPAN

Abstract

This paper presents two experimental investigations for cavitation characteristics of restriction orifices. The first experiment is about the spatial distribution of cavitation shock pressure in a pipe at the downstream of restriction orifices. The second experiment is the investigation of butterfly valve throttling to the cavitation in a multiperforated orifice installed piping.

From the results of the experiment for the cavitation shock pressure, it is concluded the maximum shock pressure remarkably increases with the decrease of cavitation number regardless of the orifice types. The maximum shock pressure becomes smallest on cone type orifice, and largest on single hole orifice. Multiperforated orifice is between this two.

The results of the experiment for occurrence of cavitation due to the interference of butterfly valve show that the cavitation occurs at a relatively high cavitation number when the multiperforated orifice is placed at 1D downstream of the butterfly valve. The butterfly valve throttling accelerates the cavitation at the multiperforated orifice because of the closed orifice installation.

1 Introduction

In the process / chemical plants, restriction orifices, such as single hole orifice, multiperforated orifice and cone type orifice are used to restrict the flow in the piping system. Figure 1 shows three types of orifices. It is known that if severe cavitation occurs at piping in which the restriction orifice is installed, the trouble such as pipe vibration, noise and pipe erosion may occur. For the restriction orifices, there are some investigations concerning the cavitation characteristics on the pipe vibration and noise for above three types of orifice (Tullis (1973), Numachi (1960), Fruman (1985), Kugou (1996)). Those investigation results can be used to design the restriction orifices avoiding the pipe vibration and noise induced by cavitation. But there are few investigations concerning the pipe erosion due to cavitation. It could be considered that the pipe erosion is caused by the impact or fatigue destruction due to the shock pressure that produced by the collapse of cavitation bubbles. Therefore, the spatial distribution of cavitation shock pressure inside the pipe at the downstream of restriction orifices is examined by using the pressure detecting film that is fixed in pipe with film holder. Using the looped water piping system where the restriction orifice is installed, the experiment is carried out.

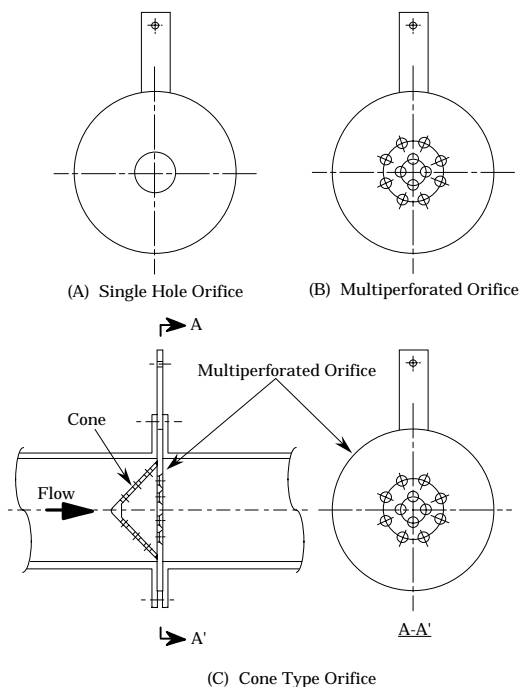


Figure 1 Restriction Orifices

Severe cavitation at a restriction orifice can be avoided by appropriate design using the investigation results for the cavitation characteristics of restriction orifices. However, at the restriction orifice which is designed taking the

cavitation into account, severe cavitation may occur due to the interference of valve throttling or elbow which is installed at upstream of a restriction orifice. In order to confirm the occurrence of cavitation due to interference of a butterfly valve by an experiment, and to investigate the countermeasure to avoid such cavitation, the piping vibration is measured changing the location of the multiperforated orifice at 1D, 3D, and 5D downstream of the butterfly valve (D : pipe inside diameter).

In these experiments, the spatial distributions of cavitation shock pressure and pipe vibrations are measured against the cavitation number, K, defined by the following equation.

$$K = \frac{P_{d1} - P_v}{\frac{1}{2} \rho \cdot v_0^2} \tag{1}$$

- where, K : cavitation number [-]
 P_{d1} : static pressure just at downstream of orifice [Pa]
 P_v : vapor pressure of fluid [Pa]
 ρ : density of fluid [kg/m³]
 v_0 : mean velocity through orifice hole [m/s]

2 Experimental Facility

Both experiments are carried out using 3 inch looped water piping system. Figure 2 shows the experimental facility. Figure 3 and 4 show the test section for the experiment of shock pressure distribution (Experiment-1) and the interference of butterfly valve (Experiment-2), respectively.

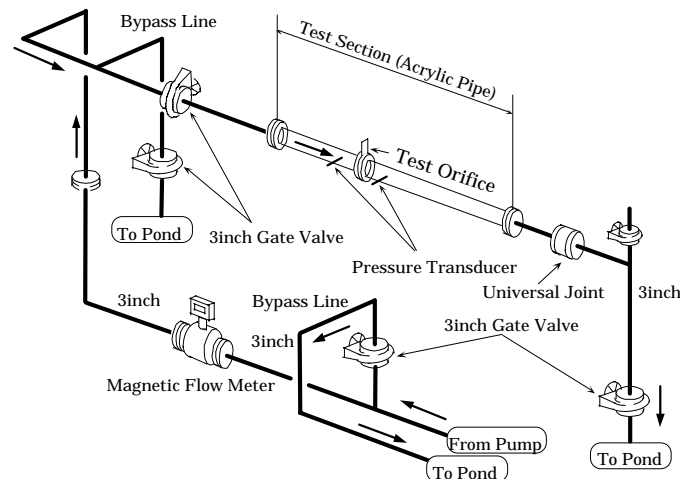


Figure 2 Experimental Facility

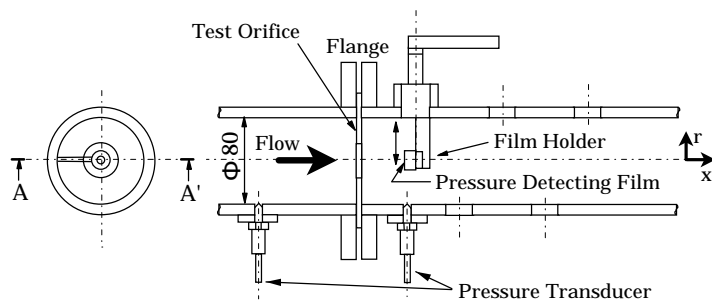


Figure 3 Test Section for Experiment-1

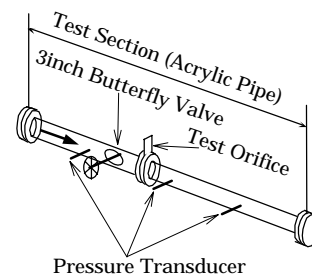


Figure 4 Test Section for Experiment-2

The water which is pumped up from a test pond by a centrifugal pump (0.0278m³/s x 0.78 MPa), flows through the 3 inch vinyl chloride piping, goes to the test section via a magnetic flow meter, and returns into the test pond.

3 Experiment-1

3.1 Method of Experiment

For Experiment-1 (experiment for cavitation shock pressure), the test section is 1.4m in length, 80mm in inside diameter and is made of the transparent acrylic pipe to observe the aspect of the cavitation. Table 1 shows the specification of the test orifices used in this experiment. The test orifice is installed at the test section, and the holder for pressure detecting film (hereinafter, referred as “film holder”) can be installed inside the pipe at 0.5D, 1.0D, 1.5D, 2.0D and 2.5D downstream of the test orifice. Figure 5 shows the illustration of film holder. The film holder is the device to fix the pressure detecting film inside the pipe. The spatial distributions of cavitation shock pressure are measured using the pressure detecting film changing the location of the film holder and the head of film holder. The pressure detecting film can show the received pressure by density of red color.

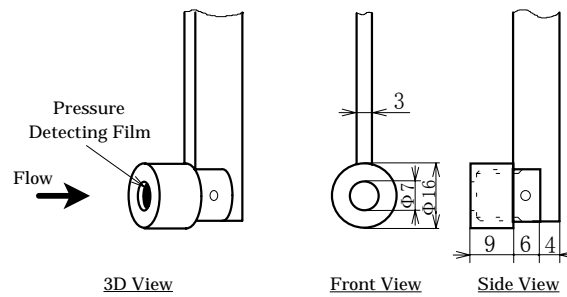


Figure 5 Illustration of Film Holder

Table 1 Specification of Test Orifices

Type of Orifice	Single Hole	Multiperforated	Cone Type
Pipe Size	3 inch	3 inch	3 inch
Ratio of equivalent orifice inside diameter to pipe inside diameter	0.37	0.37	0.37 *

* : ratio of orifice area to pipe inside sectional area of cone = 0.4

In this experiment, flow rates, pressures and spatial distributions of cavitation shock pressure are measured for 3 types of orifice shown in Table 1. Table 2 shows the specification of measuring instruments. The pressures are measured at 1D upstream and 0.5D downstream of the orifice with the pressure transducers of strain gauge type and the flow rate is measured with the magnetic flow meter.

Table 2 Specification of Instruments

Instrument	Model No.	Maker	Specifications
Pressure Transducer	PGM-2KC -10KC	KYOWA	Rated Output: 0.2MPa (PGM-2KC) 1.0MPa (PGM-10KC)
Magnetic Flow Meter	AM208	YOKO GAWA	Accuracy : +-0.1% of Span (0-20%) +0.5% of Rate (20-100%) Flow Rate Range : 0-180m ³ /h
Pressure Detecting Film	PRESCALE	FUJI FILM	Pressure Range : 0.5 - 2.5MPa (Super Low Pressure) 1.0 - 10MPa (Low Pressure) 7.0 - 25MPa (Middle Pressure) 20 - 70MPa (High Pressure)

3.2 Results of Experiment

(a) Single Hole Orifice

Figures 6 and 7 show the spatial distributions of cavitation shock pressure inside the pipe at the cavitation number, $K=1.4$ and $K=0.4$, respectively. In these figures, the vertical axis shows the radial distance of shock pressure measuring point from orifice center, and the horizontal axis shows the axial distance of shock pressure measuring point from orifice center, and the distributions of cavitation shock pressure.

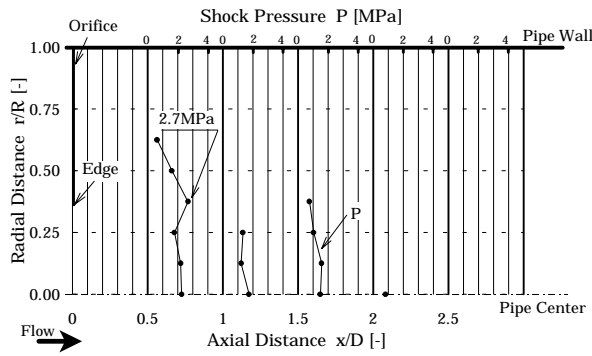


Figure 6 Shock pressure distribution (single hole, $K=1.4$)

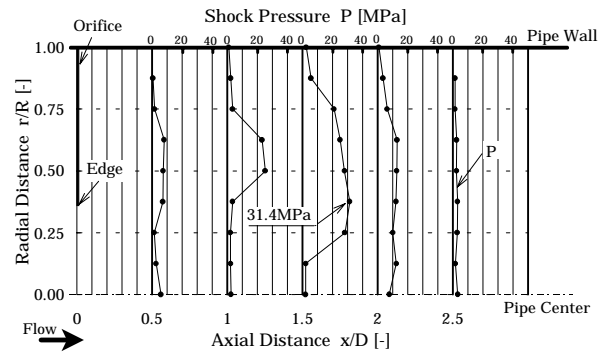


Figure 7 Shock pressure distribution (single hole, $K=0.4$)

From Figures 6 and 7, the followings are observed.

- (1) There is a point where the cavitation shock pressure becomes maximum at the downstream of orifice edge (radial distance of measuring point, $r/R = 0.375$). It could be considered that this phenomenon occurs because the cavitation bubbles generated near the orifice edge flows to downstream and collapses at the area in which the static pressure recovers. The large shock pressure is due to the collapse of the cavitation bubbles.
- (2) When the cavitation becomes severer (the cavitation number, K becomes smaller), the sphere in which the large shock pressure is observed becomes wider in radial and axial direction, and the cavitation shock pressure becomes larger. It could be considered that this phenomenon occurs because the amount of cavitation bubbles becomes more and the sphere in which the static pressure recovers, extends to the downstream.

(b) Multiperforated Orifice

Figures 8 and 9 show the spatial distributions of cavitation shock pressure inside the pipe at the cavitation number, $K=0.8$ and $K=0.4$, respectively. For the multiperforated orifice, the shock pressure exceeding 0.5 MPa (lower limit of pressure detecting film) is not observed at any point at the cavitation number, $K > 0.8$.

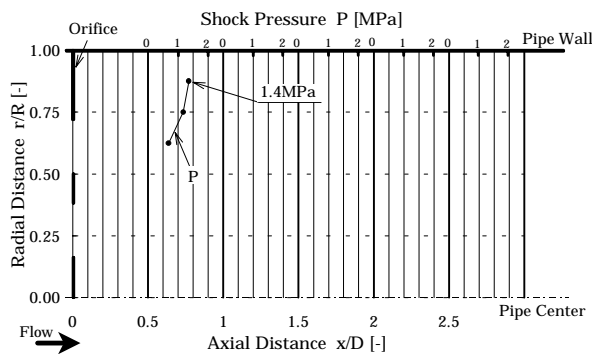


Figure 8 Shock pressure distribution (multiperforated, $K=0.8$)

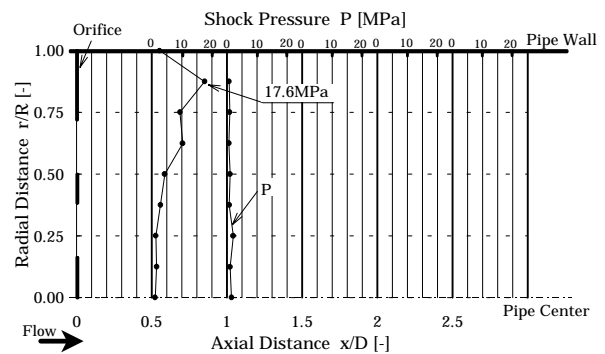


Figure 9 Shock pressure distribution (multiperforated, $K=0.4$)

From Figures 8 and 9, the followings are observed.

- (1) There is a point where the cavitation shock pressure becomes maximum near the pipe wall (radial distance of measuring point, $r/R = 0.875$). It could be considered that the cavitation shock pressure becomes lower at the center of the flow because of the interference of the cavitation bubbles from orifice edges, and becomes larger near the pipe wall because of less interference of the cavitation bubbles.
- (2) When the cavitation becomes severer, the sphere in which the large shock pressure is observed becomes wider in radial direction, and the cavitation shock pressure becomes larger.

(c) Cone Type Orifice

Figures 10 and 11 show the spatial distributions of cavitation shock pressure inside the pipe at the cavitation number, $K=0.6$ and $K=0.4$, respectively. For the cone type orifice, the shock pressure exceeding 0.5 MPa is not observed at any point at the cavitation number, $K > 0.6$.

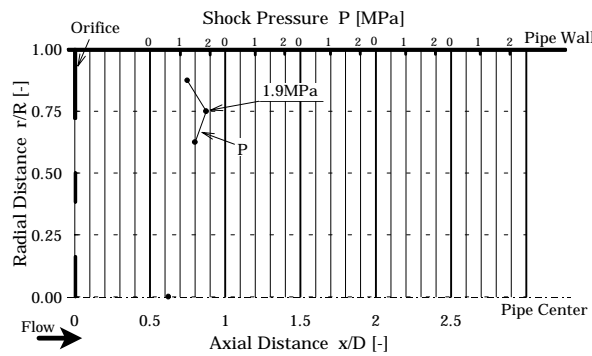


Figure 10 Shock pressure distribution (cone type, $K=0.6$)

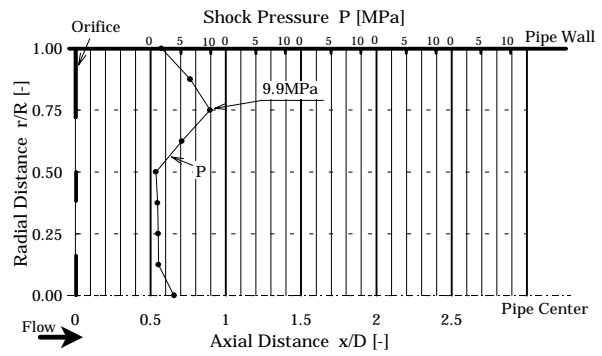


Figure 11 Shock pressure distribution (cone type, $K=0.4$)

From Figures 10 and 11, the followings are observed.

- (1) There is a point where the cavitation shock pressure becomes maximum near the pipe wall (radial distance of measuring point, $r/R = 0.75$). It could be considered that this phenomenon occurs because of same reason for the multiperforated orifice. The maximum shock pressure is observed inner region in comparison with the multiperforated orifice because the flow has the vector to the pipe center due to the cone.
- (2) When the cavitation becomes severer, the sphere in which the large shock pressure is observed becomes wider in radial direction, and the cavitation shock pressure becomes larger.

(d) Maximum Shock Pressure

Figure 12 shows the relation between the maximum shock pressure, P_{MAX} and the cavitation number, K . Table 3 shows the maximum shock pressure at the pipe wall, P_{WMAX} at $K = 0.4$ (severest cavitation condition in the experiment).

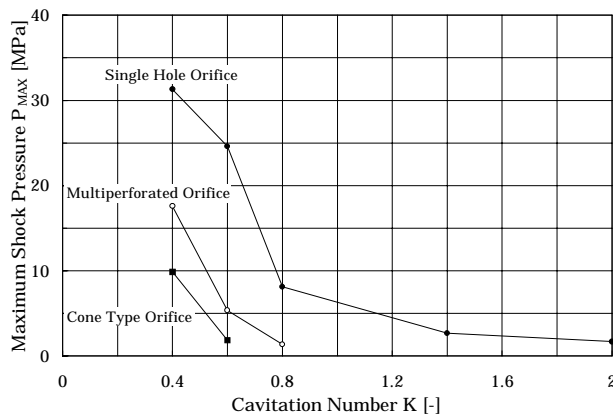


Figure 12 Maximum shock pressure versus cavitation number

Table 3 Maximum Shock Pressure at Pipe Wall

Orifice Type	Maximum Shock Pressure at Pipe Wall P_{WMAX} [MPa]	Detected Position on Axial Direction	Cavitation Number, K [-]
Single Hole	2.5	1.5D	0.4
Multiperforated	2.6	0.5D	0.4
Cone Type	1.8	0.5D	0.4

From Figures 12 and Table 3, the followings are observed.

- (1) The maximum shock pressure remarkably increases with decrease of the cavitation number regardless of the orifice types.
- (2) The maximum shock pressure becomes smallest on the cone type orifice, and largest on single hole orifice. The multiperforated orifice is between this two.
- (3) The maximum shock pressures at the pipe wall become almost same on single hole orifice and multiperforated orifice, and the smallest on the cone type orifice. The maximum shock pressures at the pipe wall are much lower than that at the inside of the pipe.

4 Experiment-2

4.1 Method of Experiment

For Experiment-2 (experiment for occurrence of cavitation due to interference of butterfly valve), the test section is 1.3m in length, 80mm in inside diameter and is made of the transparent acrylic pipe to observe the aspect of the cavitation. The butterfly valve is installed at the test section and the test orifice is installed at 1D, 3D and 5D downstream of the butterfly valve. Table 4 shows the specification of butterfly valve. The test orifice is 3 inches 12 holes multiperforated orifice, and the hole diameter is 8.5 mm.

Table 4 Specification of Butterfly Valve

Type	Wafer-Type Rubber Seated Butterfly Valve (based on JIS B2032)
Size	3 inch (80 mm)
Rating Pressure	10 K (10 kgf/cm ² G)

In this experiment, flow rates, pressures and accelerations of piping vibration are measured changing the throttling of the butterfly valve, and the length between the butterfly valve and the test orifice. The pressures are measured at 1D upstream of the butterfly valve and 0.5D downstream of the orifice with the pressure transducers of strain gauge type and the flow rate is measured with the magnetic flow meter. The accelerations of piping vibration are measured at 0.5D downstream of the test orifice and treated using the FFT spectrum analyzer within the frequency range from 1 Hz to 5 kHz, and the root mean square (r.m.s.) values " a_{rms} " are obtained.

4.2 Results of Experiment

Figures 14 to 16 show the relation between the acceleration of piping vibration, α'_{rms} and the cavitation number, K for the 1D, 3D and 5D of length between butterfly valve and test orifice, respectively. In these figures, the vertical axis shows the acceleration of piping vibration, α'_{rms} which is defined by the following formulae.

$$\alpha'_{rms} = \text{ratio between the r.m.s value of acceleration of piping vibration and total specific energy at upstream of orifice}$$

$$= \frac{\alpha_{rms}}{\frac{P_u}{\rho} + \frac{V^2}{2}} \quad [1/m] \quad (2)$$

where, α_{rms} : r.m.s. value of the acceleration of piping vibration [m/s²]
 P_u : upstream pressure of the orifice [Pa]
 V : mean pipe velocity [m/s]

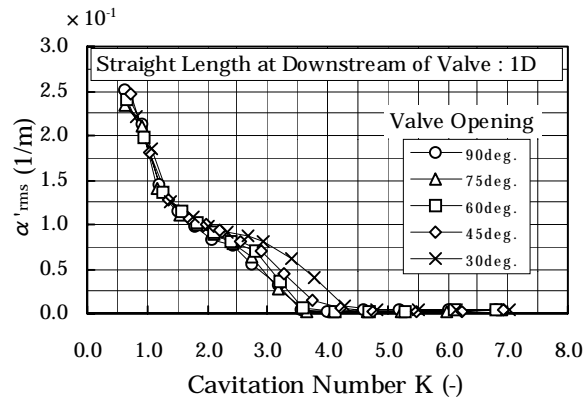


Figure 13 Acceleration of piping vibration versus cavitation number (Length between the butterfly valve and the test orifice = 1D)

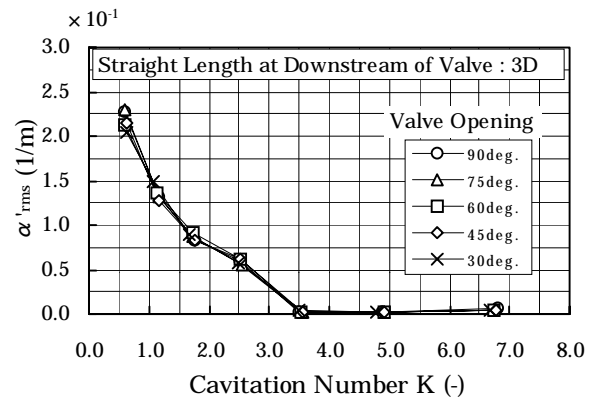


Figure 14 Acceleration of piping vibration versus cavitation number (Length between the butterfly valve and the test orifice = 3D)

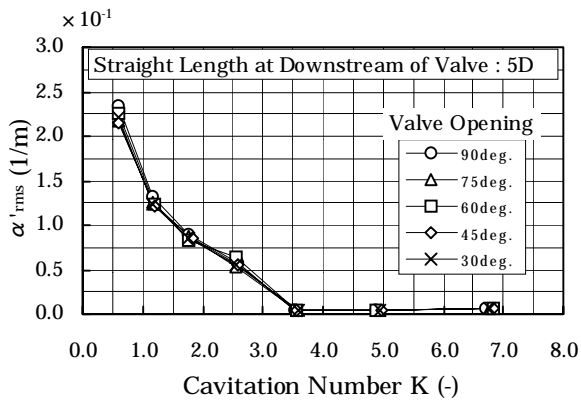


Figure 15 Acceleration of piping vibration versus cavitation number (Length between the butterfly valve and the test orifice = 5D)

From Figure 13, the followings are observed for 1D length between the butterfly valve and the test orifice.

- (1) The relations between the piping vibration and the cavitation number are almost same for over 60 degree of the opening of butterfly valve.
- (2) The incipient cavitation number (piping vibration starts to increase at this cavitation number) becomes larger as the opening of the butterfly valve becomes smaller.
- (3) When the opening of the butterfly valve is 30 degree, the piping vibrations at around $K = 3$ to 4 become large in comparison with that for other larger valve openings.
- (4) The cavitation occurs at a relatively high cavitation number. The butterfly valve throttling accelerates the cavitation at the multiperforated orifice because of the closed orifice installation.

From Figures 14 and 15, the followings are observed for 3D and 5D lengths between the butterfly valve and the test orifice.

- (1) The relations between the piping vibration and the cavitation number are almost same regardless of the opening of the butterfly valve.
- (2) The incipient cavitation number is about $K_i = 3.5$ regardless of the opening of the butterfly valve.

5 Conclusion

From the results of the experiment for the cavitation shock pressure, it is concluded that : (1)The characteristics of the distribution of cavitation shock pressure vary with the orifice types at low cavitation number. The maximum shock pressure is observed at the downstream of orifice edge on single hole orifice and near the piping wall on multiperforated and cone type orifice. (2)The maximum shock pressure remarkably increases with the decrease of cavitation number regardless of the orifice types. The maximum shock pressure becomes smallest on cone type orifice, and largest on single hole orifice. Multiperforated orifice is between this two.

The results of the experiment for occurrence of cavitation due to the interference of butterfly valve show that the cavitation occurs at a relatively high cavitation number when the multiperforated orifice is placed at 1D downstream of the butterfly valve. The butterfly valve throttling accelerates the cavitation at the multiperforated orifice because of the closed orifice installation.

References

- Fruman, D. H., Rousseau, A., and Nienaltowska, E., 1985, "Critical Cavitation Numbers of Multiperforated Plates", *ASME, Fluids Engineering Division*, 153-160
- Kugou, N., Matsuda, H., Izuchi, H., Miyamoto, H., Yamazaki, A., Ogasawara, M., 1996, "Cavitation Characteristics of Restriction Orifices (Experiment on Characteristics of Piping Vibration and Noise)", *ASME, Fluids Engineering Division Summer Meeting*, Vol. 236, No. H01072-1996, 457-462
- Numachi, F., Yamabe, M., and Oba, R., 1960, "Cavitation Effect on the Discharge Coefficient of the Sharp-Edged Orifice Plate", *ASME Journal of Basic Engineering*, 1-11
- Tullis, J. P., Asce, M., and Govindarajan, R., 1973, "Cavitation and Size Scale Effects for Orifices", *ASCE Journal of the Hydraulic Division*, Vol.99, No. HY3, 417-430